European Archives of Oto-Rhino-Laryngology (2019) 276:1783–1791
https://doi.org/10.1007/s00405-019-05409-5

HEAD & NECK

Endoscopic anatomical study of the trans-lateral molar approach to the infratemporal fossa

Wei-wei Cai[1] · Yan Zou[2] · Zhuang Kang[2] · Jian-gang Liang[1] · Hai-yong He[3] · Qin-tai Yang[4]

Received: 20 January 2019 / Accepted: 25 March 2019 / Published online: 3 April 2019

Abstract

Background The infratemporal fossa (ITF) is located deep in the skull base. Recently, the endoscopic transoral approach has enabled maxillofacial surgeons to access the ITF using a less invasive approach compared to the traditional transfacial and endonasal endoscopic approaches.

Objective The present study aims to provide maxillofacial surgeons with new data concerning direct endoscopic measurement and precise anatomical topography features of the endoscopic trans-lateral molar approach to ITF by comparing the endoscopic and regional anatomy of ITF. A clinical case receiving the proposed surgical approach is used to determine the feasibility of this technique.

Method The anatomical data were obtained by measuring the bone anatomical landmarks and analyzing the CT imaging data using GE's Advance Windows 4.1 software on 25 subjects (50 sides). Morphological pictures of the regional anatomy and endoscopic anatomy were obtained from 6 (12 sides) adult cadaver heads, and the anatomical features were described. The present study reports the management of one case using the proposed surgical approach.

Results The proposed surgical approach clearly revealed neurovascular, muscular, and surgical landmarks in the ITF. The surgical case supports the minimally invasive treatment approach, which could rapidly access the ITF and completely excise benign tumors.

Conclusion The anatomical studies and surgical case presentation helps us understand the spatial relationship of surgical landmarks of the surgical approach to the ITF for the treatment of benign lesions in the deep cranial base area.

Keywords Endoscope · Regional anatomy · Surgical approach · Lateral molar · Pterygopalatine fossa · Infratemporal fossa

Introduction

The infratemporal fossa (ITF) is located in the anterior part of parapharyngeal space and contains important neurovascular vessels. Anatomically, ITF is surrounded by complex craniofacial structures such as the maxillary sinus (anterior), middle cranial fossa (superior), ramus of the mandible (lateral), and the nasopharynx (mesial) [1, 2]. Due to the complex anatomy and involvement of vital structures, the surgical management of ITF tumors, which account for about 0.5% of head and neck tumors (> 82% are benign tumors and resistant to radiotherapy) [3, 4], is challenging for surgeons.

The use of the endoscopic endonasal approach to the pterygopalatine fossa (PPF) and ITF has enabled maxillofacial surgeons to accumulate anatomical data to improve the surgical management of various pathological lesions in the ITF using endoscopic approaches [5–8]. However, in the case of the endoscopic endonasal approach, the surgeon

Wei-wei Cai, Yan Zou, Hai-yong He and Qin-tai Yang contributed equally to this work.

✉ Hai-yong He
jlhhy007@126.com

✉ Qin-tai Yang
yang.qt@163.com

[1] Department of Otolaryngology-Head and Neck Surgery, Panyu Central Hospital, Guangzhou 511400, Guangdong, China

[2] Department of Radiology, The Third Affiliated Hospital, Sun Yat-sen University, Guangzhou 510630, Guangdong, China

[3] Department of Neurosurgery, The Third Affiliated Hospital, Sun Yat-sen University, No. 600 Tianhe Road, Tianhe District, Guangzhou 510630, Guangdong, China

[4] Department of Otolaryngology-Head and Neck Surgery, The Third Affiliated Hospital, Sun Yat-sen University, No. 600 Tianhe Road, Tianhe District, Guangzhou 510630, Guangdong, China

still has to deal with nerve vessels in the PPF before entering the ITF [5–9]. In addition, it is difficult to treat tumors located deep in the posterior and inferior part of ITF near the angulus mandibulae [8, 10–12]. Recent studies describing the endoscopic transoral approach to ITF for the treatment of ITF lesions have led to the neurosurgeons being interested in this quicker, less invasive approach to the maxilla and neurovascular vessels in the PPF [5, 13, 14]. The aim of the anatomic anatomical study is to quantify (through radiological measurement and topographical photographs of endoscope and regional anatomy) the associated anatomic landmarks in ITF that the surgeon could obtain while safely approaching this region through the lateral molar route using an endoscope. In addition, we apply the anatomical basis and present a clinical case using the proposed surgical approach to support the feasibility of this technique.

Materials and methods

The present study was approved by the institutional ethical review board of Third Affiliated Hospital, Sun Yat-sen University, Guangzhou, China (Ref: 2018 02-428-01). All procedures were performed in accordance with the ethical standards of the institutional and national research committees and the 1964 Helsinki Declaration. All patients in this study signed the informed consent form for allowing use of their clinical data for research purposes.

MSCT scanning and measurements

The present study included the MSCT data of 25 adults who attended the Third Affiliated Hospital of Sun Yat-sen University, Guangzhou, China for CT examination of sinus from April 2018 to June 2018. Each MSCT scan of nasal sinuses was performed using the QX/I spiral CT machine (GE Medical Systems; Milwaukee, USA) and fixed scanning settings (tube voltage: 120 kV, tube current: 230 mA, layer thickness: 2.5 mm, matrix 512 × 512, bulb rotation speed: 0.8 s/round, scan mode HQ mode Pitch = 3, bed speed: 3.8 mm/rot and scan field of view 25 cm). The CT scanned images data were transferred to the Advantage Workstation for Diagnostic Imaging System (AWDIS Version 4.1). The data were used for the multiplanar reconstructions (slice thickness of 1.25 mm and a slice spacing of 0.4 mm) calculating the distance of the bony surgical landmarks. The bone three-dimensional (3D) rendering images were observed for the specific relationship of bony surgical landmarks with various orientation views of ITF.

Analysis of 3D volume rendering images of ITF (Fig. 3a–c) showed that the bony landmarks were located on the medial of mandibular and the skull base. The anatomical landmarks associated with ITF included the foramen rotundum (FR), foramen ovale (FO), foramen spinosum (FS), foramen lacerum (FL), carotid canal (CC), and lingula mandible (LM).

To attain a relatively constant anatomical relationship, the measurement points were defined on maxillary and mandibular second molars. We set the first measurement point at the posterolateral edge of the maxillary second molar and measured the distance to the landmarks on the skull base (Table 1). The second measurement point was set as the posterolateral edge of the mandibular second molar to measure the distance to LM, the landmarks located on the mandibular (Table 1). As the FO lies on the most anterior part of the ITF's ceiling while the endoscope is approaching the ITF, it was set as an anatomical reference point for the measurement of other anatomic landmarks on the ceiling of ITF (Table 2).

Anatomical observations

The endoscopic and local anatomical observations were performed on six adult cadaver heads (twelve sides) provided by the Department of Anatomy, Sun Yat-sen University, Guangzhou, China.

Table 2 Distance (millimeter) between the foramen ovale (FO) and each of the anatomic landmark ($n = 50$)

	Min	Max	Mean	Standard deviation
FS	3.91	13.54	9.44	2.61
FR	14.62	20.30	18.00	1.54
FL	7.59	17.87	12.35	2.50
CC	12.51	29.80	19.37	3.83

FS foramen spinosum, *FR* foramen rotundum, *FL* foramen lacerum, *CC* carotid canal

Table 1 Distance (millimeter) from the posterior lateral margin of the root of the second upper and lower molar to each anatomical landmark ($n = 50$, $\bar{x} \pm s$)

	LM	FR	FO	FS	CC
SSM	–	42.26 ± 5.68	41.74 ± 5.68	44.33 ± 5.81	50.13 ± 5.84
ISM	26.72 ± 4.31	–	–	–	–

SSM superior second molar, *ISM* inferior second molar, *FO* foramen ovale, *FR* foramen rotundum, *FS* foramen spinosum, *CC* carotid canal

Endoscopic anatomy

For endoscopic anatomical observations, the cadaver heads were fixed on the operation table and the oral cavity was opened widely using a Boyle–Davis gag. Anatomical observations were performed using the following steps.

First, a longitudinal incision was made on the mucosa lateral to the mandibular molars, exposing the surface of the medial side of the mandible. To locate the LM, it is necessary to keep the mucosa stripper adhering to the surface of the medial mandible to create access to ITF when separating the mucosa. We ensured that the buccal nerve was positioned from the posterior to anterior direction and adhered to the lateral wall of the maxilla. The buccal nerve can reach the gap between the upper and lower pterygoid muscles.

Second, the fat pad between the medial surface of mandible and the medial pterygoid muscle was partly removed and the scalpel remained close to the mandible's surface. For identifying the LM, the inferior alveolar artery in turn can be used to track the main trunk of internal maxillary artery (IMA). The inferior alveolar nerve can be tracked from the mandibular foramen to the medial of lateral pterygoid muscle and from the foramen ovale in the skull base joining the main trunk of mandibular nerve.

Third, the inferior alveolar nerve can reach the lower pterygoid muscle (LPM), and the inferior alveolar artery can track to the main trunk of the IMA.

Lastly, the round foramen (foramen rotundum) can be found in the medial part of the pterional root. The maxillary nerve exits the middle cranial base through the round foramen. The excision of the lateral pterygoid muscle (LPM) from the root of pterygoid process may explore the mandibular nerve corresponding to the position of foramen ovale. The foramen spinosum and the middle meningeal artery entering into middle cranial fossa can be adjacent to the foramen ovale.

Regional anatomy of ITF

First, a facial skin incision was used to excise the parotid gland, facial nerve, masseter muscle, and (to expose the zygomatic arch) the mandibular neck and coronoid process. The temporal muscle attached to the mandibular coronoid was inverted following the partial excision of zygomatic arch and mandibular ramus. Then, the lateral wall of ITF was exposed. The fats in the pterygopalatine space were then removed to expose the LPM, medial pterygoid muscle (MPM), the branch of IMA, and the branch of the mandibular nerve. Finally, the LPM was removed to reveal the root of the mandibular nerve, the middle meningeal artery.

Clinical case report

Clinical data and preoperative examination

A 65-year-old female patient attended the Department of Neurosurgery, The Third Affiliated Hospital of Sun Yat-sen University, Guangzhou, China complaining of paroxysmal pain in the left side inferior alveolar nerve that had persisted for the last 3 years. The pain was lightning-like, 2–4 times a day, and each episode lasted for a few seconds. The patient reported that facial movements such as tooth brushing, talking, and blowing triggered the pain without inducing any dizziness, nausea, vomiting, or headache.

During the clinical examination, the patient was conscious and fully cooperative. Pupils in both sides were equal in size (3 mm) and the reflection of pupils was sensitive to light. The facial symmetry was maintained while frowning or during mouth opening or tongue movements. Sensory feelings in the left side of the face were weaker compared to the contralateral side. The radiological examination (spiral CT and MRI) revealed the presence of a radiopaque mass (measuring approximately 34×35 mm) in the ITF. The CT images of the tumor showed low to intermediate attenuation and adjacent mandibular bone remodeling with smooth corticated edges (Fig. 1a–c). The MRI revealed clear boundaries of the left ITF mass, low signal of T1W (Fig. 1), high signal of T2W1, and mixed with a few patchy low signals. The MRI (T1W1-enhanced scan) showed that the tumor had obvious enhancement of lesion edges and division (Fig. 1g–i). The MRI and CT findings suggested that the lesion of ITF was likely a schwannoma of the inferior alveolar nerve.

Surgical procedure of the case

Before the surgical procedure, surgeons at the Department of Vascular Surgery Interventional Radiology were on standby to manage any complications associated with the rupture of the internal carotid artery. The surgical procedure was performed using orotracheal intubation with the patient in the supine position under general anesthesia. Following disinfection of the skin, the oral cavity was widely opened using a Boyle–Davis gag (Fig. 2b). Under the 0-degree 4-mm endoscope (Karl Storz, Tuttlingen, Germany), the mandibular buccal mucosa was incised to access the tumor through the mandible with coblation (Arthrocare ENT Coblator II, Sunnyvale, CA, USA) (Fig. 2c).

Clinically, the lesion was capsulated, showed clear boundaries and solid texture, and had invaded the lower part of the jaw occupying the bulb shape posterior to the mandibular molars (Fig. 2d, e). After incising the capsule of the tumor, the inner part of the mass was ablated in bulk (Fig. 2f). The tumor was shrunk and separated through the

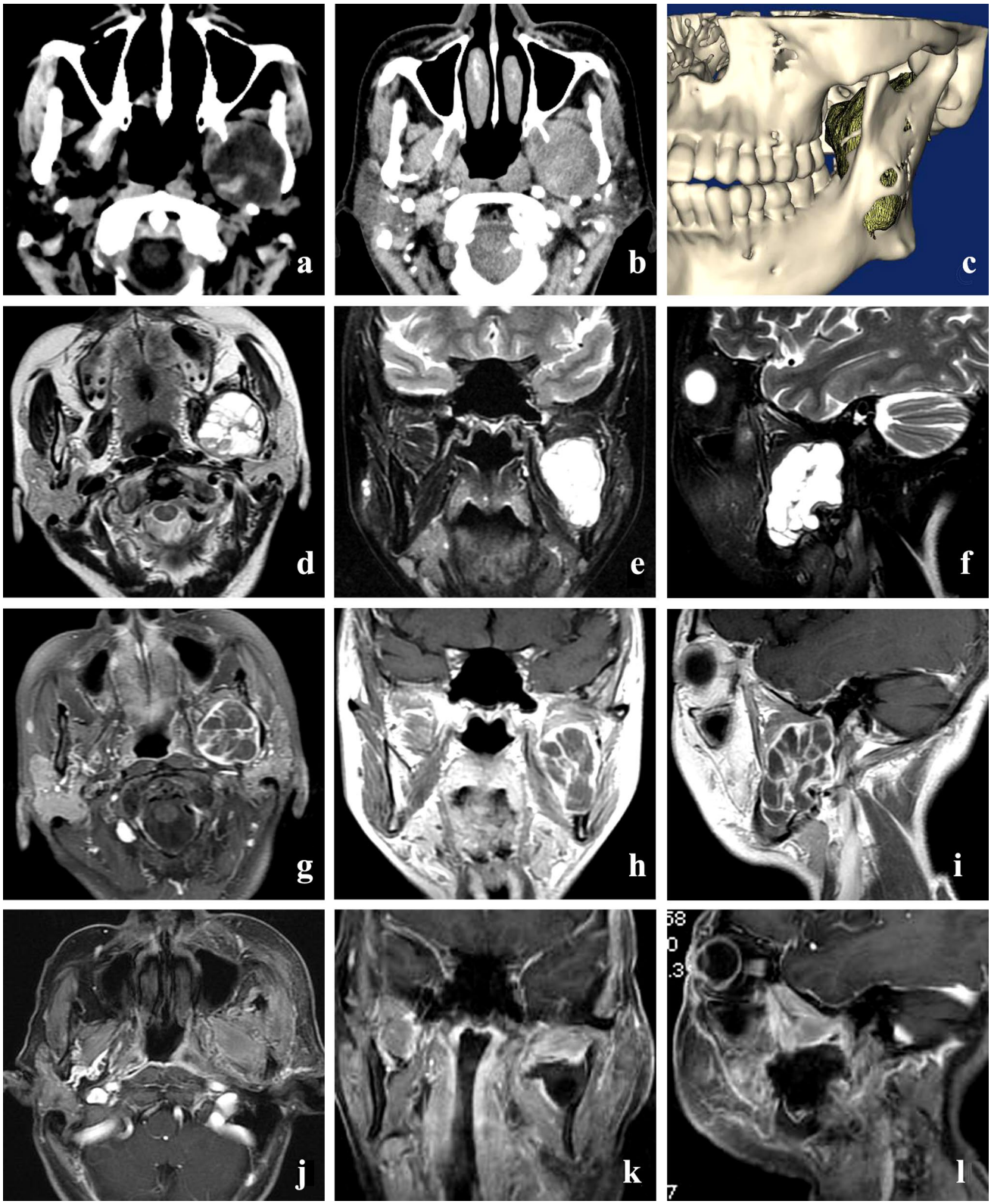

ITF (Fig. 2g, f). A 0° endoscope was used to ensure that no residue remained. After hemostasis, the defect was filled with gelatin using a sponge and sutured using the absorbable sutures (2/0 absorbable polyglycolic acid braid, OPTIME®, Péters Surgical) (Fig. 2i, j). The patient was then given post-operative instructions and discharged.

◂**Fig. 1** The CT and Magnetic resonance imaging (MRI) data of the presented case showing the infratemporal fossa pathology. **a** Coronal view of CT scan. **b** Coronal view of CT enhanced scan shows that there is a clear boundary between the tumor and the internal carotid artery. **c** CT (bone)—MRI-T2 (tumor) fusion volume three-dimensional reconstruction. The tumor grows expansively, the mandible is partially destroyed, and the tumor extends from the lower part of the mandible. **d**, **e** and **f** (MRI-T2 scan of the tumor in ITF. The border of tumor is clear, and there is no obvious adhesion between the parotid gland and the tumor. **g**, **h** and **i** Enhanced MRI-T1 scan of the head showed the lesion encapsulated and the wall enhanced, leading to the destruction of the mandible. **j**, **k** and **l** The postoperative head MRI-T1 enhanced scan showed that the tumor completely resected without any residual lesions

Results

Bone structures of ITF

The distance between the second measurement point and lingular mandible (LM) was approximately 26.7 mm, (Fig. 3c, Table 1), which helped in locating the inferior alveolar nerve and artery behind LM.

The anatomical landmarks on the ceiling of ITF include the FO and FS. The associated anatomic landmarks are the carotid canal and foramen lacerum (Fig. 3b). The distance from the first measurement point to these landmarks and the distance between FO and FS as well as CC and FL can help to know the depth of the operation on the cranial base and the spatial relationship with the internal carotid artery (Tables 1, 2, Fig. 3b). The FO is located at the top of the infratemporal fossa and extends backward into the inferior surface of lateral skull base area, which consists of temporal bone and the great wing of the sphenoid bone. The CC is located about an average distance of 19.3 mm behind the FO, and the distance between the CC and the lateral root of the second upper molar is about 50 mm (Tables 1, 2, Fig. 3b). The connecting line of FO–FS and the mandibular ramus (green line in Fig. 3b) is roughly parallel to the connecting line of FL–CC (Fig. 3b).

The comparative observations between endoscopic and regional anatomy observations of ITF

After resection of the LPM, the regional anatomic image of ITF presents the IMA lying on the nervus mandibularis from the lateral view (Fig. 5b). The endoscopic image in Fig. 5a shows the branches of mandibular nerve including inferior alveolar nerve, lingual nerve (LN), and buccal nerve (BN) lying orderly on the surface of the MPM from back to front of the medial wall of ITF (Fig. 5a, c). The pterygoid muscles from the scapular sulcus to the mandibular angle form the inner wall of the gap (Fig. 5c).

The trunk of the mandibular nerve in the ITF is characterized by the top-down approach. The main trunk of the internal maxillary artery runs from the posterior to anterior ITF and the branches diverge (Fig. 5b–d). The endoscope showed that the lateral wall of ITF is a relatively fixed structure, which consisted of the medial side of the mandible and the part of temporal muscle attaching to the coronoid process and the mandibular notch (Fig. 5c). This characteristic requires that the operation process (entering ITF) should lean against the surface of the lateral wall of ITF with tracking of the IAN from the LM to avoid injuring the IMA.

Results of surgery

Following the operation, the patient reported no infections or any other complications, and the paroxysmal pain originating from the left inferior alveolar space completely disappeared. The surgical incision healed appropriately without showing any signs of inflammation. The histopathological examination of the excised lesion confirmed the diagnosis as schwannoma. The MRI findings at the postoperative follow-up visit after 3 months showed complete removal of the tumor and there were no signs of recurrence (Fig. 2j–l).

Discussion

Multiple endoscopic approaches (transnasal and transoral) to the ITF have been reported in the literature. [5–14] Of these approaches, only the endoscopic trans-lateral maxilla approach (reported as the endoscopic transvestibular paramandibular approach) to the ITF can attain a full view of the ITF without creating the surgical corridor through bony structures such as maxilla and pterygoid processes of the sphenoid. [8, 11–13].

In the present study, we made a series of measurements between the different anatomical landmarks in the ITF to give surgeons a conception of the size of this region when the endoscope approaches through the trans-lateral molar route (Tables 1 and 2). In this way, we try to improve the surgeon's orientation during exposure of this area with anterior aspect from endoscopic anatomy, lateral aspect from regional anatomy, and the endoscope approach orientation illustration.

From a neurosurgical point of view, the value of using anatomical knowledge of the ITF in endoscopy is that if the approach can attain an excellent view of the ITF, seeing the anatomical landmarks can help to prevent internal carotid artery injury while showing the type of lesions.

The endoscopic trans-lateral molar approach enables an endoscopic view of the ITF without excision of all other nasal cavity and maxilla structures, which could interfere with the physiology of the nasal cavity [7, 8] (Figs. 4c, 5c, d). We set a relatively constant anatomical landmark (the second molar as the measurement point) to help in

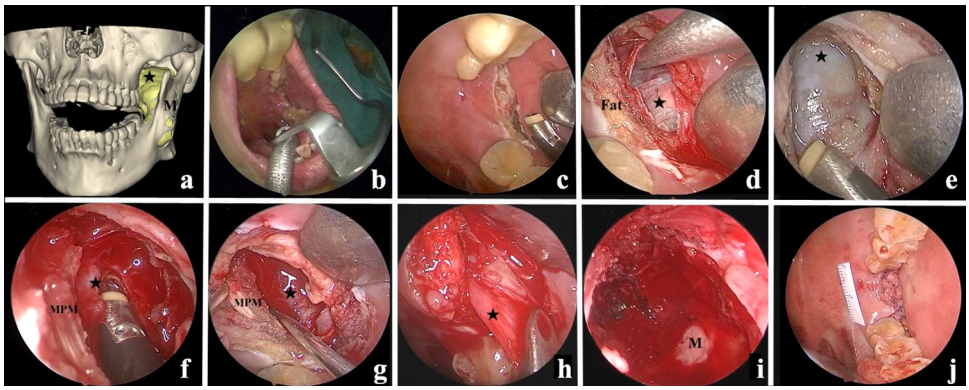

Fig. 2 **a** Open mouth CT-MR fusion mass showing the posterior lateral space of the molar used to access the tumor. **b** The patient's position before surgery. The mouth was kept open with a Boyle–Davis gag. **c** The surgical incision is located on the mucosa of the lateral molar. **d** 0° endoscopic view of the tumor and the surface fascia and bone. **e** The fascia and surrounding bone are exposed, and the tumor capsule is intact. **f** Resection of the central tissue of the cyst, reducing the volume of the tumor. **g** After the volume of tumor was reduced, the tumor is separated from the surrounding tissue. **h** The intact capsule is completely removed. **i** The 0° endoscopic view of the tumor cavity after removing the tumor. **j** Absorbable suture of the incision. Fat: fat. Star: tumor. *MPM* medial pterygoid muscle, *M* mandibular

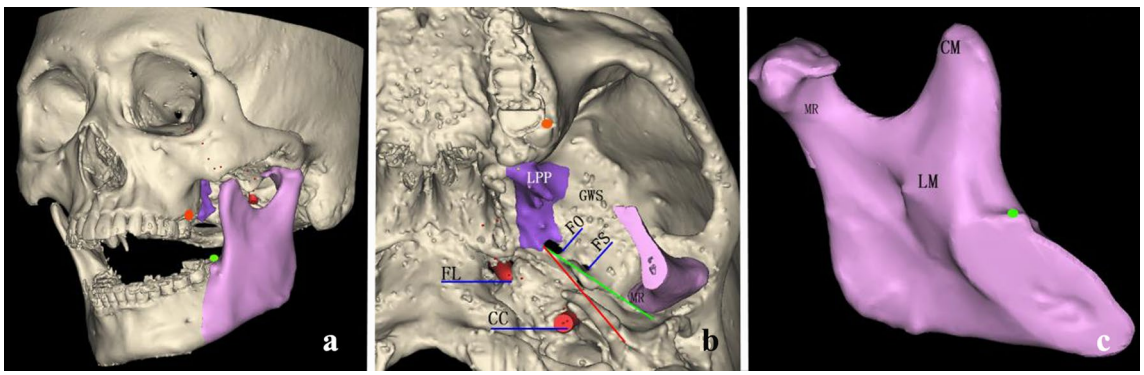

Fig. 3 The boundaries and associated anatomical landmarks of infratemporal fossa (ITF); **a** The facial view showing the buccal surface of ramus of mandible (pink lavender), **b** The ceiling of ITF showing the relationship of various landmarks. **c** The lingual view of the ramus of mandible: the mandibular ramus (MR). Deep purple: medial boundary of ITF, lateral pterygoid plate (LPP). Superior boundary of ITF, greater wing of sphenoid bone (GWS) and part of the squamous–temporal bone. **a** Bony anatomical landmark of the ITF. Foramen ovale (FO), foramen spinosum (FS), coronoid process of the mandible (CM), foramen lacerum (FL), opening of internal carotid canal (CC), lingula mandible (LM), mandibular foramen (MF). Red spot: the first measurement point. Green point: the second measurement point. Green line: the connection of FO–FS–MR. The lateral side of the safety line is a safe area; red line: the connection of FO–styloid process. To avoid the injury of internal carotid atery, the warning line should not be strided over

identifying the spatial relationship with other bony landmarks on the skull base, such as endoscopic endonasal anatomic studies that set the nasal columella as the measurement point during management of deep lesions in the skull base [9, 15, 16].

The lingula mandible is a critical landmark located on the medial surface of the posterior mandibular (Fig. 3c). Our results showed how a mean distance of 26.72 mm between the lateral posterior of the second inferior molar and lingula mandible can be used to locate the inferior alveolar nerve. Hence, the lingula mandible is commonly used as the key point for administering regional anesthesia [17, 18].

Clinically, the lingula mandibular can also be found by finger palpation to locate the entrance of inferior alveolar nerve into the mandible foramen just behind the lingula mandible. Additionally, the inferior alveolar nerve can be used to track the foramen ovale. The foramen ovale is located at the superior surface of the ITF, which is one of the most important anatomical landmarks associated with ITF surgeries. [7, 8, 13].

Although the present study showed the endoscopic trans-lateral molar approach to be safer in providing direct access to the ITF (compared to the endoscopic endonasal approach), there are still several potential risks associated with this approach.

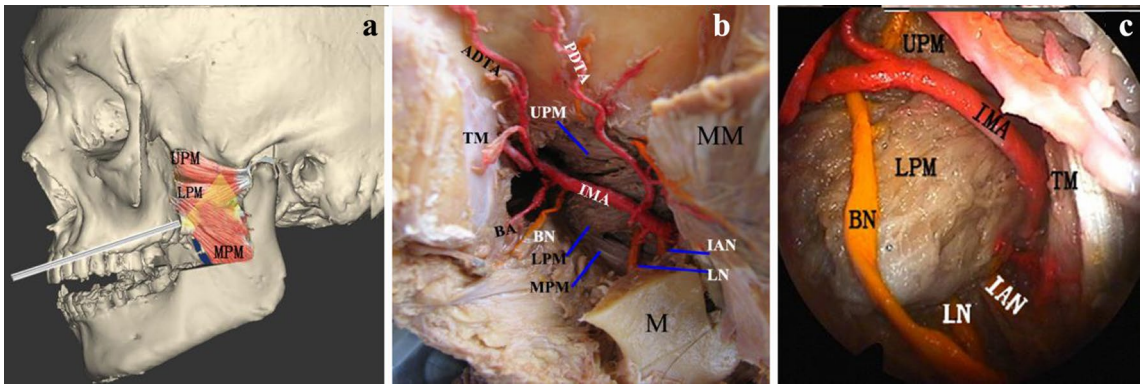

Fig. 4 **a** The virtual endoscopic view of the trans-lateral molar to infratemporal fossa (ITF) and the lateral regional anatomical view. **b** The regional anatomy of the ITF. **c** The 0° endoscopic view of ITF shows the nerves, blood vessels, and muscles inside the left ITF. Lateral pterygoid plate (LPP), the superior alveolar nerve (SAN), the infraorbital artery (IOA), buccal nerve (BN), internal maxillary artery (IMA), deep anterior temporal artery (ADTA), deep posterior temporal artery (PDTA), inferior alveolar nerve (IAN), lingual nerve (LN), up, head of the pterygoid (UPM), down, head of the pterygoid muscle (DPM), temporal muscle (TM), masseter muscle (MM), buccal artery (BA), and mandible (M)

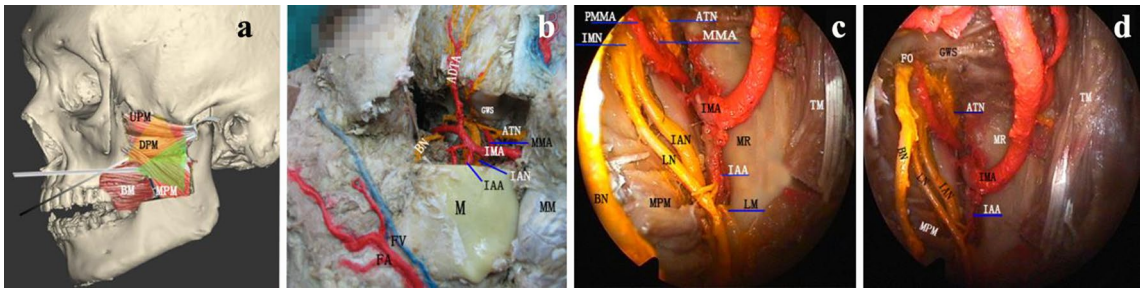

Fig. 5 The virtual endoscopic view of the trans-lateral molar to infratemporal fossa (ITF) and the lateral regional anatomical view. The green area corresponds to the endoscopic view field in **c** and the yellow area corresponds to the endoscopic view field in **d**. **b** The regional anatomy in ITF shows the distribution of neurovascularity. **c** The 0° endoscopic view of the ITF after removing the lateral pterygoid muscle. **d** The 0° endoscopic view of the ceiling of the ITF. Up, head of the pterygoid (UPM), down, head of the pterygoid muscle (DPM), medial pterygoid muscle (MPM), buccal muscle (BM), masseter muscle (MM), mandible (M), maxillary artery (IMA), middle meningeal artery (MMA), para-meningeal artery (PMMA), inferior alveolar artery (IAA), inferior alveolar nerve (IAN), lingula mandible (LM), mandibular ramus (MR), foramen ovale (FO) and auriculotemporal nerve (ATN)

First, hemostasis in the narrow space should be appropriately managed. In our surgical experience, hypothermia plasma ablation can effectively control the bleeding of small arteries and the pterygoid plexus of veins. The major arteries such as the internal maxillary artery (IMA) and inferior alveolar artery (IAA) should be clipped using long endoscopic clip applicators and the IMA can be ligated if necessary. The IAA can be identified beside the lingula mandible and tracked to the trunk of internal maxillary artery (Fig. 5d).

Second, a good anatomical knowledge of the vertical segment of the internal carotid artery (ICA) in relation to parapharyngeal space and ITF is essential. The tensor veli palatini muscle and solid fascia separate the parapharyngeal space from the ITF. Therefore, injury to the veli palatini muscles or fascia may lead to fatal bleeding during the endoscopic surgical process [19, 20].

According to the anatomical data, it is approximately 50 mm from the maxillary second molar to the opening of ICA and the distance from the FO to ICA is 20 mm (Tables 1 and 2). According to MSCT imaging data, ICA running in the temporal bone is according to the connection between the foramen lacerum and the opening of ICA at the skull base (Fig. 3b). To keep the operative range within safe limits (Fig. 3b), attention to the anatomical landmarks (FO, FS, and MR) as reference points of surgical depth would help in avoiding potential injury to the ICA. Moreover, a team of vascular surgery interventional radiologists should be involved if necessary.

Finally, as it is difficult to dissect neurovascular tissues in a muscular space composed of muscles that include the lateral pterygoid muscle, the medial pterygoid muscle, part of the temporalis, and medial surface of the mandible (Fig. 4b, c), skill is necessary to find the lingula mandible, which can

identify the inferior alveolar nerve and the posterior inferior alveolar artery and lead to the trunk of mandibular nerve and internal maxillary artery.

Following the anatomical studies and surgical case presentation, we suggest that this approach has the potential to conveniently access the ITF compared to the endonasal endoscopic approaches via the maxillary and PPF to ITF. For example, bony walls of the maxilla and the nerve and vessel layers in PPF [6, 7] are not distorted, hence significantly reducing the operating time and intraoperative bleeding.

Compared to the endoscopic transoral-transpharyngeal approach to ITF[5], the trans-lateral molar approach to ITF may avoid the pterygoid plate, medial pterygoid muscle, styloglossus muscle and ascending palatine artery before entering the ITF.

Another advantage of trans-lateral molar approach is that it includes better access to the surgical field due to bypassing of the maxillary and pterygoid process. Additionally, this approach can expose the ceiling of ITF and the lower part (the mandibular angle) of the ITF with the 0° endoscope (Fig. 5a, c, d) thus facilitating easy access with surgical instruments. The disadvantage of using the endonasal endoscopic approach to the ITF is difficulty in attaining a suitable endoscopic view of the lower part of the ITF around the mandibular angle, especially in the case of a poorly pneumatized maxilla.

On the other hand, limitations of the endoscopic trans-lateral molar approach to the ITF include needing a surgical retractor following the incision in the buccal mucosa (Fig. 3c) to keep the access open and establish a passage between the lateral of the molar and the medial of the mandible. In addition, similar to any other endoscopic approaches to the ITF, this approach needs effective management to control bleeding in the muscular spaces to improve endoscopic vision and decrease operating time.

In the present study, we reported only one clinical case with a short follow-up period using the proposed surgical approach. Hence, further clinical studies are required to validate this approach for future clinical applications.

Conclusion

The anatomical studies and surgical case presented here have provided anatomical data of the endoscopic trans-lateral molar approach to the ITF which may help in providing safe and accurate surgical management of pathological lesions in this anatomically complex area.

Acknowledgements Data collection was conducted in The Third Affiliated Hospital, Sun Yat-sen University. The dissection of cadaver heads was performed in the Anatomic Lab of The Third Affiliated Hospital, Sun Yat-sen University. Other works including CT image processing, anatomic measurement, and article writing were conducted in Panyu Central Hospital.

Compliance with ethical standards

Conflict of interest The authors have no funding, financial relationships, or conflicts of interest to disclose.

References

1. Isolan GR, Rowe R, Al-Mefty O (2007) Microanatomy and surgical approaches to the infratemporal fossa: an anaglyphic three-dimensional stereoscopic printing study. Skull Base 17:285–302
2. Hitotsumatsu T, Rhoton AL Jr (2000) Unilateral upper and lower subtotal maxillectomy approaches to the cranial base: microsurgical anatomy. Neurosurgery 46:1416–1452 **(discussion 1452–1413)**
3. Kuet ML, Kasbekar AV, Masterson L, Jani P (2015) Management of tumors arising from the parapharyngeal space: a systematic review of 1,293 cases reported over 25 years. Laryngoscope 125:1372–1381
4. Riffat F, Dwivedi RC, Palme C, Fish B, Jani P (2014) A systematic review of 1143 parapharyngeal space tumors reported over 20 years. Oral Oncol 50:421–430
5. Dallan I, Fiacchini G, Turri-Zanoni M, Seccia V, Battaglia P, Casani AP et al (2016) Endoscopic-assisted transoral-transpharyngeal approach to parapharyngeal space and infratemporal fossa: focus on feasibility and lessons learned. Eur Arch Otorhinolaryngol 273:3965–3972
6. Theodosopoulos PV, Guthikonda B, Brescia A, Keller JT, Zimmer LA (2010) Endoscopic approach to the infratemporal fossa: anatomic study. Neurosurgery 66:196–202 **(discussion 202–193)**
7. Alfieri A, Jho HD, Schettino R, Tschabitscher M (2003) Endoscopic endonasal approach to the pterygopalatine fossa: anatomic study. Neurosurgery 52:374–378 **(discussion 378–380)**
8. Taylor RJ, Patel MR, Wheless SA, McKinney KA, Stadler ME, Sasaki-Adams D et al (2014) Endoscopic endonasal approaches to infratemporal fossa tumors: a classification system and case series. Laryngoscope 124:2443–2450
9. Fortes FS, Sennes LU, Carrau RL, Brito R, Ribas GC, Yasuda A et al (2008) Endoscopic anatomy of the pterygopalatine fossa and the transpterygoid approach: development of a surgical instruction model. Laryngoscope 118:44–49
10. Van Rompaey J, Suruliraj A, Carrau R, Panizza B, Solares CA (2013) Access to the parapharyngeal space: an anatomical study comparing the endoscopic and open approaches. Laryngoscope 123:2378–2382
11. Battaglia P, Turri-Zanoni M, Dallan I, Gallo S, Sica E, Padoan G et al (2014) Endoscopic endonasal transpterygoid transmaxillary approach to the infratemporal and upper parapharyngeal tumors. Otolaryngol Head Neck Surg 150:696–702
12. Lee JT, Suh JD, Carrau RL, Chu MW, Chiu AG (2017) Endoscopic Denker's approach for resection of lesions involving the anteroinferior maxillary sinus and infratemporal fossa. Laryngoscope 127:556–560
13. Chan JY, Li RJ, Lim M, Hinojosa AQ, Boahene KD (2011) Endoscopic transvestibular paramandibular exploration of the infratemporal fossa and parapharyngeal space: a minimally invasive approach to the middle cranial base. Laryngoscope 121:2075–2080
14. Patwa HS, Yanez-Siller JC, Gomez Galarce M, Otto BA, Prevedello DM, Carrau RL (2018) Analysis of the far-medial transoral

endoscopic approach to the infratemporal fossa. Laryngoscope 128:2273–2281
15. Solari D, Magro F, Cappabianca P, Cavallo LM, Samii A, Esposito F et al (2007) Anatomical study of the pterygopalatine fossa using an endoscopic endonasal approach: spatial relations and distances between surgical landmarks. J Neurosurg 106:157–163
16. Cai WW, Zhang GH, Yang QT, Wang ZY, Liu X, Ye J et al (2010) Endoscopic endonasal anatomy of pterygopalatine fossa and infratemporal fossa: comparison of endoscopic and radiological landmarks. Zhonghua Er Bi Yan Hou Tou Jing Wai Ke Za Zhi 45:843–848
17. Gamieldien MY, Van Schoor A (2016) Retromolar foramen: an anatomical study with clinical considerations. Br J Oral Maxillofac Surg 54:784–787
18. Palti DG, Almeida CM, Rodrigues Ade C, Andreo JC, Lima JE (2011) Anesthetic technique for inferior alveolar nerve block: a new approach. J Appl Oral Sci 19:11–15
19. Fortes FS, Pinheiro-Neto CD, Carrau RL, Brito RV, Prevedello DM, Sennes LU (2012) Endonasal endoscopic exposure of the internal carotid artery: an anatomical study. Laryngoscope 122:445–451
20. Muto J, Carrau RL, Oyama K, Otto BA, Prevedello DM (2017) Training model for control of an internal carotid artery injury during transsphenoidal surgery. Laryngoscope 127:38–43